



Review

Ultrasmall Superparamagnetic Particles of Iron Oxide and Cardiac Magnetic Resonance: Novel Imaging in Everyday Conditions

Vasiliki Tsampasian ^{1,2} , Ioannis Merinopoulos ^{1,2}, Donnie Cameron ^{1,3}, Pankaj Garg ^{1,2} 
and Vassilios S. Vassiliou ^{1,2,*}

- ¹ Norwich Medical School, University of East Anglia, Norwich NR4 7TJ, UK; vasiliki.tsampasian@nnuh.nhs.uk (V.T.); ioannis.merinopoulos@nnuh.nhs.uk (I.M.); donnie.cameron@uea.ac.uk (D.C.); p.garg@uea.ac.uk (P.G.)
- ² Department of Cardiology, Norfolk and Norwich University Hospital, Norwich NR4 7UY, UK
- ³ C. J. Gorter MRI Center, Department of Radiology, Leiden University Medical Centre, 2333 ZA Leiden, The Netherlands
- * Correspondence: v.vassiliou@uea.ac.uk

Abstract: Myocardial inflammation has been hypothesised to be the common underlying mechanism through which several cardiovascular diseases develop and progress. Cardiac magnetic resonance (CMR) has become a powerful non-invasive tool that enables the direct visualisation of the myocardium. The emerging use of ultrasmall superparamagnetic particles of iron oxide (USPIO) and their magnetic properties is gaining a lot of research interest. USPIO-enhanced CMR can provide valuable information, as it allows for the identification of active inflammation in the myocardium, a process that has been hypothesised to be the substrate for adverse remodelling and, eventually, heart failure. In this review, we summarise the properties of USPIO and their role in cardiac magnetic resonance imaging as well as their clinical applications.

Keywords: ultrasmall superparamagnetic particles of iron oxide (USPIO); cardiac magnetic resonance (CMR); iron oxide nanoparticles



Citation: Tsampasian, V.; Merinopoulos, I.; Cameron, D.; Garg, P.; Vassiliou, V.S. Ultrasmall Superparamagnetic Particles of Iron Oxide and Cardiac Magnetic Resonance: Novel Imaging in Everyday Conditions. *Appl. Sci.* **2022**, *12*, 6913. <https://doi.org/10.3390/app12146913>

Academic Editor: Julio Garcia Flores

Received: 19 May 2022

Accepted: 6 July 2022

Published: 8 July 2022

Publisher's Note: MDPI stays neutral with regard to jurisdictional claims in published maps and institutional affiliations.



Copyright: © 2022 by the authors. Licensee MDPI, Basel, Switzerland. This article is an open access article distributed under the terms and conditions of the Creative Commons Attribution (CC BY) license (<https://creativecommons.org/licenses/by/4.0/>).

1. Introduction

A deeper understanding of cardiovascular disease has shifted the research interest towards the investigation of pathophysiological processes that encompass myocardial energetics and metabolism. Naturally, cardiovascular imaging has advanced incrementally to allow the non-invasive investigation of such processes and important features beyond anatomy and morphology that determine the biological foundation behind disease pathogenesis and progression.

Myocardial inflammation has a central role in the pathogenesis of various cardiovascular diseases. Although an important mechanism of tissue healing and recovery, the persistence of inflammation may lead to pathological and adverse cardiac remodelling [1]. Therefore, it may drive pathological processes that lead to the pathogenesis of a plethora of diseases such as dilated cardiomyopathy, ischaemic cardiomyopathy, and heart failure with a reduced or preserved ejection fraction [2,3]. Macrophages have a vital role both in the initiation and maintenance of inflammation and in the tissue repair mechanisms following an acute insult [4,5]. Therefore, the early identification of macrophage activity will enable the early detection and monitoring of a variety of diseases and may allow the steering of therapeutic management strategies towards appropriate pathways.

Cardiac magnetic resonance (CMR) imaging offers significant advantages such as a high spatial resolution, tissue characterisation, and the avoidance of harmful radiation and invasive tests [6]. With the use of advanced methods and techniques, such as late

gadolinium enhancement (LGE) and T1 and T2 mapping, myocardial oedema and inflammation can be detected. However, these sequences do not allow for the identification of inflammation at a cellular level. For that reason, the use of ultrasmall superparamagnetic particles of iron oxide (USPIO) has been successfully implemented in CMR studies and has so far offered a valuable means of detecting and evaluating cellular inflammation [7–9]. USPIO-enhanced CMR is a powerful imaging technique that may reveal information vital to the diagnosis and management of cardiovascular diseases.

2. Iron Oxide Nanoparticles

Iron oxide nanoparticles were first introduced as liver-specific MRI contrast agents [10–12]. Since then, however, their application has been successfully expanded in the rapidly developing field of cardiac and vascular imaging [6,7,9,13]. Iron oxide nanoparticles are naturally found in the environment and as matter in air pollution and volcanic eruptions [14]. Superparamagnetic iron oxide nanoparticles may be generated as emissions from industry and power stations, but they can also be chemically synthesised through various methods [15]. These include classical synthesis by co-precipitation, reactions in constrained environments, the polyol method, flow injection synthesis, and sonolysis [14,15]. In addition, novel methods of nanoparticle synthesis have been described, such as the generation of magnetic α -Fe₂O₃/Fe₃O₄ heterogeneous nanoparticles via a facile solution combustion process and the synthesis of iron oxide nanoparticles by the rapid inductive heating method [16,17]. Their potential applications, safety, and bioavailability are mainly determined by two of their most essential characteristics: their coating and their size [7,18].

The core of these nanoparticles comprises iron oxide, more commonly magnetite (Fe₃O₄) or maghemite (γ -Fe₂O₃), and its radius ranges between 5 and 15 nm [19,20] (Figure 1). Iron oxide itself is hydrophobic; hence, the nanoparticles are usually modified with an external coating formed of a biocompatible hydrophilic polymer such as dextran or polyethylene glycol [7,21]. This coating is essential in order to prevent the opsonisation (i.e., binding with plasma proteins) of the nanoparticles, which would unavoidably occur in the bloodstream without it [19,21]. Additionally, through electrostatic interactions, the coating also inhibits the aggregation of nanoparticles that would otherwise take place due to their hydrophobic properties [19]. Another important consideration is an excess of iron ions may lead to the overproduction of reactive oxygen species or free radicals and subsequently cause protein, lipid, and DNA damage and, finally, cellular apoptosis [22]. Thus, the other critical ‘task’ of the external coating is to provide a stable cover that prevents the oxidation of the iron and its subsequent harmful effects, allowing the safe use of the nanoparticles [22]. Apart from the above, the coating that surrounds the core of the nanoparticle also acts like a ‘harbour’ to which ligands, drug molecules, and other molecular targets can bind [6]. Taking all of these into consideration, it is obvious why molecular imaging and targeted drug delivery are some of the areas where iron oxide nanoparticles have been successfully applied [23–25].

According to their size, iron oxide particles can be grouped into four different categories: very small superparamagnetic particles of iron oxide (VSPIO, diameter < 20 nm), ultrasmall superparamagnetic particles of iron oxide (USPIO, diameter 20–50 nm), small superparamagnetic particles of iron oxide (SPIO, diameter 20–250 nm), and micro-sized particles of iron oxide (MPIO, diameter 1–8 μ m) [6,7]. However, the vast majority of the proposed applications for iron oxide nanoparticles use small and ultrasmall particles with diameters of 50 nm or less [6].

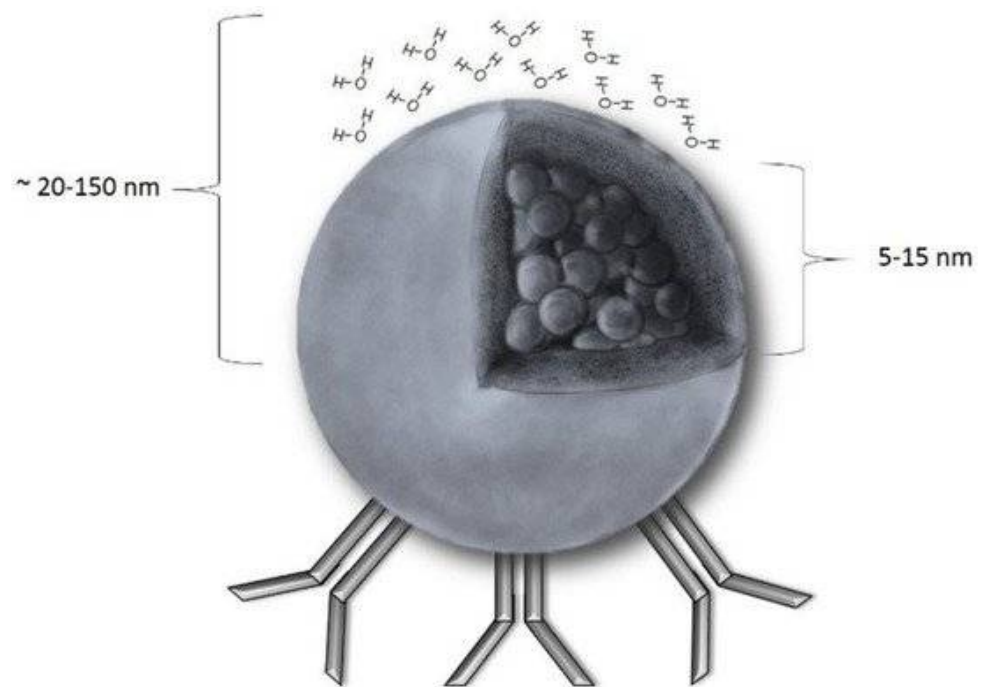


Figure 1. A schematic presentation of a SPION (superparamagnetic iron oxide nanoparticle): The core radius ranges from 5 to 15 nm, and the hydrodynamic radius (core with shell and water coat) is between 20 and 150 nm. Unless there is a magnetic field, magnetisation equals 0. As shown, SPIONs can be easily coupled with antibodies that facilitate the majority of the SPION applications discovered so far [19]. Reproduced with permission from Dulińska-Litewka et al. [19] under a Creative Commons Attribution 4.0 International License.

The concept of the superparamagnetism of nanoparticles was expressed for the first time almost a century ago [26]. The magnetic nanoparticles induce local magnetic field inhomogeneities through which water molecules will diffuse, leading to the magnetic relaxation of the water protons, from which image contrast is generated [27]. Iron oxide particles form crystalline structures that contain multiple iron ions [28]. Sufficiently large crystal-containing regions constitute a magnetic domain that comprises thermodynamically independent particles that have a net magnetic dipole that is larger than the total of the individual unpaired electrons [28]. In the absence of a magnetic field, these domains have no net magnetic field; however, in the presence of an external magnetic field, the magnetic domains are reoriented, and the net magnetic moment of the particle surpasses that of the paramagnetic ions [27,28]. This phenomenon is called superparamagnetism and appears in small ferromagnetic or ferrimagnetic nanoparticles as a result of their small size and crystalline nature, both of which are required for this phenomenon to occur [7,28,29].

3. Iron Oxide Nanoparticles (USPIO) and Inflammation

USPIO accumulate at sites of inflammation; therefore, their detection with CMR allows for the identification of active myocardial inflammation. Following intravenous administration, the iron oxide nanoparticles remain in the intravascular space and are taken up by the macrophages of the reticuloendothelial system [20]. Both the size and the coating of the nanoparticles are crucial for their bio-availability, with the smaller and more hydrophilic particles being a lot less susceptible to phagocytosis [6,23]. While larger iron oxide nanoparticles are rapidly identified and engulfed by the macrophages in the lymphoreticular organs (liver, spleen, lymph nodes), USPIO, because of their smaller size, are much less readily recognised and can subsequently avoid instant phagocytosis [6]. In this way, USPIO remain in the bloodstream for much longer, as reflected by their longer half-life (up to 36 h) compared to larger iron oxide nanoparticles (up to 2 h) [6,27]. After being taken up by macrophages, they are subsequently carried by these cells to areas

of active inflammation [7]. In addition to this mechanism, it has also been suggested that iron oxide nanoparticles passively cross the endothelial barrier at sites of loss of integrity and with increased permeability [7,30]. It has been shown, however, that the main mechanism by which USPIO accumulate is predominantly via cellular infiltration within the myocardium [31].

USPIO-tagged macrophages have been identified with MRI in murine models of myocardial ischaemia and infarction [32,33]. In a proof-of-principle trial that consisted of fourteen patients with acute myocardial infarction, it was shown that USPIO have the ability to detect infiltrating macrophages, identifying areas of active inflammation [30]. In another proof-of-concept study that included sixteen patients with acute myocardial infarction, USPIO uptake was evident in areas of the infarcted and remote myocardium [34]. More recently, Lagan et al. demonstrated that USPIO can identify areas of myocardial inflammation in a murine model, with USPIO having been shown to be present inside macrophages in areas of the infarcted myocardium [1]. The same study, however, also showed that USPIO can accumulate in areas of inflammation not only after being engulfed by the macrophages but can also be 'passively' present in the interstitium outside phagocytic cells [1]. This is a significant finding, as it shows that USPIO detection is not specific for macrophage activity, and therefore, the cardiac MRI techniques used should be able to differentiate USPIO enhancement due to active macrophage uptake from the passive presence of the nanoparticles in the myocardial interstitium [1].

4. The Impact of the Iron Oxide Nanoparticles on CMR Imaging

By altering the relaxation properties of the surrounding hydrogen protons and changing the apparent proton density of the surrounding tissue, iron oxide nanoparticles influence the local magnetic resonance properties. Their use is associated with shorter T2 values and hypointense regions on T2- and T2*-weighted images [23,28]. Several factors can affect the signal intensities on T2* sequences, such as the presence of oedema or haemorrhage. For this reason, the impact of USPIO accumulation can only be evaluated with the careful examination of pre- and post-contrast images of the area of interest [13]. Typically, patients are therefore subjected to two consecutive CMR scans, with the second one being 24 h after USPIO administration [35]. More recently, it was shown that multi-time-point (at 50 and 75 h post-contrast administration) multiparametric CMR helped differentiate active USPIO uptake from macrophages from passive tissue distribution [1].

Their impact of iron oxide nanoparticles and, more specifically, USPIO can be quantified by measuring the changes in the T2* and R2* values ($R2^* = 1/T2^*$) [1,7]. Uniformly dissolved USPIO alter the relaxation rates, including the R1 (longitudinal magnetic resonance relaxation rate) and R2* (transverse magnetic resonance relaxation rate) [1,36]. Nevertheless, R2* particularly is sensitive to actively phagocytised USPIO, whereas R1 is not [1]. Therefore, the R2*/R1 ratio is extremely useful for differentiating the active USPIO uptake from the passively distributed USPIO [1,7]. In a study by Lagan et al., the ratio of R2*/R1 at 75 h post-USPIO administration was demonstrated to have a 90% sensitivity and 85% specificity for detecting active USPIO uptake in infarcted and remote myocardium in acute myocardial infarction and chronic ischaemic cardiomyopathy [1].

Iron oxide nanoparticles also cause T1 shortening [37,38]. However, the T1-relaxivity of iron oxides can vary substantially depending on the strength of the magnetic field, the size of the core of the nanoparticle, and the degree of the particle aggregation [7,20,39]. More specifically, the T1 shortening caused by the nanoparticles is diminished in areas with significant particle aggregation, with the opposite phenomenon observed in areas with diffusely located nanoparticles [40]. This, however, can be avoided through the use of lower-flip-angle radiofrequency pulses and longer repetition times [7].

5. Clinical Applications in Myocardial Imaging

Multiple studies have assessed the role of USPIO-enhanced CMR in ischaemic cardiomyopathy (Figure 2). In a study that included 16 patients with acute ST-segment

elevation myocardial infarction, Alam et al. demonstrated that USPIO were taken up by the infarcted myocardial tissue and, to a lesser degree, by the peri-infarct and the remote myocardium, as evidenced by increased $R2^*$ values [34]. This was in keeping with the results of an NIMINI-2 (Non-invasive Myocardial Inflammation Imaging Based on New Molecular Magnetic Resonance Imaging) study, which showed that the absolute $T2^*$ values were decreased in the infarcted myocardial zone and, again to a lesser degree, in the peri-infarct zone [30]. In the same study, ex vivo analysis revealed that USPIO uptake was detected specifically in cultured macrophages and not in the peripheral blood monocytes, supporting the theory that USPIO absorption is mainly due to their accumulation in infiltrating myocardial macrophages or their passive accumulation in areas of loss of endothelial integrity rather than their phagocytosis by peripheral macrophages that then relocate to the heart [30].

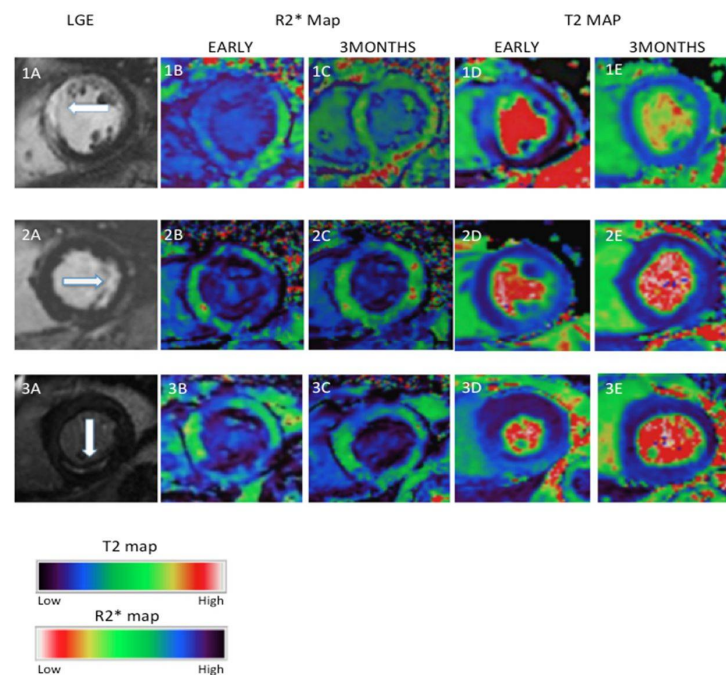


Figure 2. Examples of myocardial oedema and ferumoxytol enhancement in the infarct area after myocardial infarction (MI). Three examples of MI (1, anteroseptal, 2, lateral and 3, inferior) showing LGE on T1-weighted imaging (1A–3A), ferumoxytol enhancement ($R2^*$ maps) (1B–3B,1C–3C), and oedema (T2 maps) (1D–3D,1E–3E) at early (up to 10 days in (1B–3B,1D–3D)) and late (3 months in (1C–3C,1E–3E)) post-MI. Early inflammation and oedema seen on $R2^*$ maps (dark region) and T2 maps (light region), respectively, have improved or resolved by three months [31]. Reproduced with permission from Stirrat et al. [31] under a Creative Commons Attribution 4.0 International License.

These two proof-of-concept studies laid the foundation for further trials that followed and demonstrated that USPIO accumulation following acute myocardial infarction reflects active cellular inflammation in the myocardium [31,41]. As mentioned above, these studies showed that USPIO accumulated, albeit to a lesser degree, not only in the infarcted and peri-infarct but also in the remote myocardium, generating the hypothesis that inflammation and macrophage infiltration in the remote myocardium may lead to adverse myocardial remodelling. More recently, in a study that included patients with acute MI and with chronic ischaemic cardiomyopathy, Lagan et al. demonstrated that a USPIO-enhanced multi-parametric multi-time-point CMR methodology specifically differentiates active myocardial macrophage infiltration from the passive distribution of dissolved USPIO in the tissue interstitium [1]. Importantly, it was shown for the first time that there is persistent active inflammation, as evidenced by macrophage infiltration, both in the infarcted and the remote myocardium in the chronic phase following an MI [1]. Larger studies using USPIO-enhanced CMR are now needed to examine the potential role of active macrophage

infiltration in the pathogenesis of adverse myocardial remodelling in ischaemic cardiomyopathy. The limited available data on USPIO uptake following coronary artery bypass graft (CABG) have demonstrated that myocardial injury following CABG may be less dependent on macrophage infiltration and inflammation, as there was no correlation between USPIO uptake and high-sensitivity cardiac troponin or the cardiopulmonary bypass time [42].

USPIO-enhanced CMR has provided essential insights into the pathophysiology of Takotsubo cardiomyopathy. While it has been known that oedema and inflammation play a central role in this disease, Scally et al. demonstrated for the first time that active macrophage infiltration drives the pathological ventricular response and cellular inflammation [43,44]. Compared to control individuals, patients with takotsubo cardiomyopathy showed significant differences in the change on T2* and native T1 values at baseline (i.e., during the acute event). However, these differences were no longer evident after five months [44]. Notably, myocardial energetics as assessed by 31P-CMR spectroscopy demonstrated a markedly reduced energetic state, which persisted after five months [44].

In contrast with takotsubo cardiomyopathy, USPIO-enhanced CMR results have not shown evidence of active macrophage infiltration and USPIO accumulation in myocarditis despite evidence of myocardial oedema in native T1 mapping and extracellular volume (ECV) imaging (Figure 3) [1,45]. Although the data available are limited to a total of fifteen patients from two studies, USPIO uptake has not been demonstrated to be substantially increased in the myocardium of patients with myocarditis, even in the areas with confirmed myocardial oedema, as shown in native T1 and ECV imaging [1,45]. This highlights the fact that different pathologies trigger different pathways that may not necessarily be mediated by macrophages. In the case of myocarditis, immune cell activation may be dominated by other cell types, such as lymphocytes, for example, which could explain the absence of USPIO accumulation in the myocardium [1,45]. Additionally, in the study by Lagan et al. there was no correlation shown between USPIO uptake and native T1 values, which, as the authors mention, emphasises that myocardial oedema and macrophage infiltration do not necessarily occur simultaneously and may not be dependent on each other [1]. Nevertheless, given the limited number of patients in the abovementioned studies, it is impossible to draw firm conclusions, and further research is warranted to investigate this important aspect in detail.

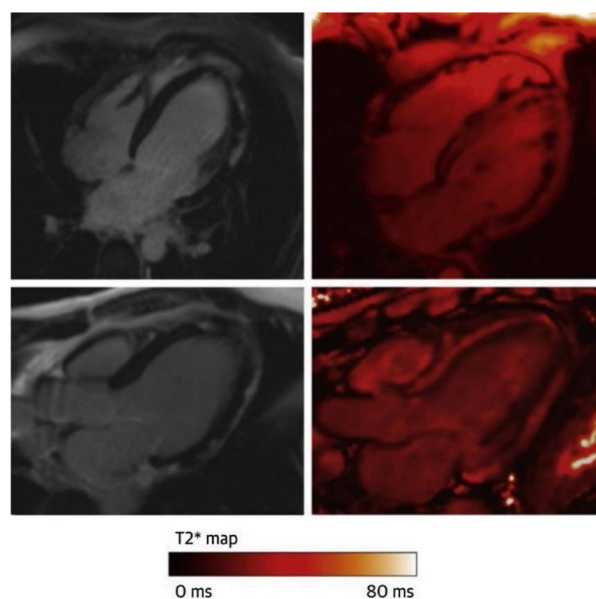


Figure 3. An example of a patient with acute myocarditis showing sub-epicardial LGE inferiorly and inferolaterally on 4-chamber and 3-chamber views (left) but no evidence of ferumoxytol uptake within the regions displaying LGE 24 h following infusion (right). CMR = cardiac magnetic resonance; LGE = late gadolinium enhancement. Reproduced with permission from Merinopoulos et al. [7].

6. Clinical Practice and Safety Profile

Ferumoxytol (Feraheme), a carboxymethyl dextran-coated USPIO, is approved for the treatment of iron deficiency anaemia in Europe and the United States. Although approved as a therapeutic agent, it is also useful as an MRI contrast agent, and as such, it is often used for research purposes under approved protocols [46].

USPIO are a safe alternative to gadolinium-based contrast agents and can even be used in patients with chronic kidney disease who are at risk of nephrogenic systemic fibrosis [47]. One of the main safety concerns is the risk of an acute hypersensitivity allergic reaction, leading the U.S. Food and Drug Administration to issue a boxed warning following 79 reported cases of anaphylaxis from an estimated total of 1.2 million injections [48]. Nevertheless, since then, large studies have successfully supported their safe use in clinical practice [46]. In a large multicentre MRI registry, in which more than 3000 patients were administered more than 4000 ferumoxytol injections, no severe or fatal adverse events occurred, while moderate adverse events were recorded in only 0.2% [47].

Over the last few years, the safety profile of USPIO has improved, and evidence from large studies further supports their application and safe use in clinical practice. Their use in CMR has successfully revealed important mechanistic pathways in which cellular inflammation and active macrophage infiltration play an important role. The research data so far reflect their successful use in the investigation of cardiac diseases and the potential that USPIO-enhanced CMR holds for use in clinical practice, to guide treatment strategies, and to be at the centre of personalised medicine.

7. Conclusions

USPIO are a safe non-invasive emerging method that can be used to evaluate myocardial inflammation by identifying active macrophage activity and infiltration. As inflammation may be an important factor driving adverse myocardial remodelling, USPIO-enhanced CMR has the potential to offer important insights into the pathophysiology of a range of cardiovascular diseases. In this way, it may become a powerful tool for risk stratification, monitoring, and targeted individualised therapeutic interventions.

Author Contributions: V.T.: original draft preparation, review and editing; I.M., review and editing; D.C., review and editing; P.G., review and editing; V.S.V., supervision, review and editing. All authors have read and agreed to the published version of the manuscript.

Funding: This research received no external funding.

Institutional Review Board Statement: Ethical review and approval were waived for this study due to it being comprehensive review of already published data.

Informed Consent Statement: Patient consent was waived as already published data were used.

Data Availability Statement: Not applicable.

Conflicts of Interest: The authors declare no conflict of interest.

References

1. Lagan, J.; Naish, J.H.; Simpson, K.; Zi, M.; Cartwright, E.J.; Foden, P.; Morris, J.; Clark, D.; Birchall, L.; Caldwell, J.; et al. Substrate for the Myocardial Inflammation–Heart Failure Hypothesis Identified Using Novel USPIO Methodology. *JACC Cardiovasc. Imaging* **2021**, *14*, 365–376. [[CrossRef](#)] [[PubMed](#)]
2. Westman, P.C.; Lipinski, M.J.; Luger, D.; Waksman, R.; Bonow, R.O.; Wu, E.; Epstein, S.E. Inflammation as a Driver of Adverse Left Ventricular Remodeling after Acute Myocardial Infarction. *J. Am. Coll. Cardiol.* **2016**, *67*, 2050–2060. [[CrossRef](#)] [[PubMed](#)]
3. Nakayama, T.; Sugano, Y.; Yokokawa, T.; Nagai, T.; Matsuyama, T.A.; Ohta-Ogo, K.; Ikeda, Y.; Ishibashi-Ueda, H.; Nakatani, T.; Ohte, N.; et al. Clinical Impact of the Presence of Macrophages in Endomyocardial Biopsies of Patients with Dilated Cardiomyopathy. *Eur. J. Heart Fail.* **2017**, *19*, 490–498. [[CrossRef](#)] [[PubMed](#)]
4. Cao, D.J. Macrophages in Cardiovascular Homeostasis and Disease. *Circulation* **2018**, *138*, 2452–2455. [[CrossRef](#)]
5. Chen, M.; Li, X.; Wang, S.; Yu, L.; Tang, J.; Zhou, S. The Role of Cardiac Macrophage and Cytokines on Ventricular Arrhythmias. *Front. Physiol.* **2020**, *11*, 1113. [[CrossRef](#)]

6. Stirrat, C.; Vesey, A.; McBride, O.; Robson, J.; Alam, S.; Wallace, W.; Semple, S.; Henriksen, P.; Newby, D. Ultra-Small Superparamagnetic Particles of Iron Oxide in Magnetic Resonance Imaging of Cardiovascular Disease. *J. Vasc. Diagn. Interv.* **2014**, *2*, 99–112. [[CrossRef](#)]
7. Merinopoulos, I.; Gunawardena, T.; Stirrat, C.; Cameron, D.; Eccleshall, S.C.; Dweck, M.R.; Newby, D.E.; Vassiliou, V.S. Diagnostic Applications of Ultrasmall Superparamagnetic Particles of Iron Oxide for Imaging Myocardial and Vascular Inflammation. *JACC Cardiovasc. Imaging* **2020**, *14*, 1249–1264. [[CrossRef](#)]
8. Tsampasian, V.; Swift, A.J.; Assadi, H.; Chowdhary, A.; Swoboda, P.; Sammut, E.; Dastidar, A.; Cabrero, J.B.; Del Val, J.R.; Nair, S.; et al. Myocardial Inflammation and Energetics by Cardiac MRI: A Review of Emerging Techniques. *BMC Med. Imaging* **2021**, *21*, 164. [[CrossRef](#)]
9. Lee, N.; Hyeon, T. Designed synthesis of uniformly sized iron oxide nanoparticles for efficient magnetic resonance imaging contrast agents. *Chem. Soc. Rev.* **2012**, *41*, 2575–2589. [[CrossRef](#)]
10. Renshaw, P.F.; Owen, C.S.; McLaughlin, A.C.; Frey, T.G.; Leigh, J.S. Ferromagnetic Contrast Agents: A New Approach. *Magn. Reson. Med.* **1986**, *3*, 217–225. [[CrossRef](#)]
11. Dias, M.H.M.; Lauterbur, P.C. Ferromagnetic Particles as Contrast Agents for Magnetic Resonance Imaging of Liver and Spleen. *Magn. Reson. Med.* **1986**, *3*, 328–330. [[CrossRef](#)]
12. Saini, S.; Stark, D.D.; Hahn, P.F.; Wittenberg, J.; Brady, T.J.; Ferrucci, J.T., Jr. Ferrite Particles: A Superparamagnetic MR Contrast Agent for the Reticuloendothelial System. *Radiology* **1987**, *162*, 211–216. [[CrossRef](#)]
13. Alam, S.R.; Stirrat, C.; Richards, J.; Mirsadraee, S.; Semple, S.I.K.; Tse, G.; Henriksen, P.; Newby, D.E. Vascular and Plaque Imaging with Ultrasmall Superparamagnetic Particles of Iron Oxide. *J. Cardiovasc. Magn. Reson.* **2015**, *17*, 83. [[CrossRef](#)]
14. Singh, N.; Jenkins, G.J.S.; Asadi, R.; Doak, S.H. Potential toxicity of superparamagnetic iron oxide nanoparticles (SPION). *Nano Rev.* **2010**, *1*, 5358. [[CrossRef](#)]
15. Wallyn, J.; Anton, N.; Vandamme, T.F. Synthesis, Principles, and Properties of Magnetite Nanoparticles for In Vivo Imaging Applications—A Review. *Pharmaceutics* **2019**, *11*, 601. [[CrossRef](#)]
16. Sharma, P.; Holliger, N.; Pfromm, P.H.; Liu, B.; Chikan, V. Size-Controlled Synthesis of Iron and Iron Oxide Nanoparticles by the Rapid Inductive Heating Method. *ACS Omega* **2020**, *5*, 19853–19860. [[CrossRef](#)]
17. Li, Y.; Wang, Z.; Liu, R. Superparamagnetic α -Fe₂O₃/Fe₃O₄ Heterogeneous Nanoparticles with Enhanced Biocompatibility. *Nanomater* **2021**, *11*, 834. [[CrossRef](#)]
18. Stirrat, C.G.; Newby, D.E.; Robson, J.M.J.; Jansen, M.A. The Use of Superparamagnetic Iron Oxide Nanoparticles to Assess Cardiac Inflammation. *Curr. Cardiovasc. Imaging Rep.* **2014**, *7*, 9263. [[CrossRef](#)]
19. Dulińska-Litewka, J.; Łazarczyk, A.; Hałubiec, P.; Szafranski, O.; Karnas, K.; Karewicz, A. Superparamagnetic Iron Oxide Nanoparticles—Current and Prospective Medical Applications. *Materials* **2019**, *12*, 617. [[CrossRef](#)]
20. Bjørnerud, A.; Johansson, L. The Utility of Superparamagnetic Contrast Agents in MRI: Theoretical Consideration and Applications in the Cardiovascular System. *NMR Biomed.* **2004**, *17*, 465–477. [[CrossRef](#)]
21. Yarjanli, Z.; Ghaedi, K.; Esmaeili, A.; Rahgozar, S.; Zarrabi, A. Iron Oxide Nanoparticles May Damage to the Neural Tissue through Iron Accumulation, Oxidative Stress, and Protein Aggregation. *BMC Neurosci.* **2017**, *18*, 51. [[CrossRef](#)] [[PubMed](#)]
22. Abakumov, M.A.; Semkina, A.S.; Skorikov, A.S.; Vishnevskiy, D.A.; Ivanova, A.V.; Mironova, E.; Davydova, G.A.; Majouga, A.G.; Chekhonin, V.P. Toxicity of Iron Oxide Nanoparticles: Size and Coating Effects. *J. Biochem. Mol. Toxicol.* **2018**, *32*, e22225. [[CrossRef](#)] [[PubMed](#)]
23. Vazquez-Prada, K.X.; Lam, J.; Kamato, D.; Xu, Z.P.; Little, P.J.; Ta, H.T. Targeted Molecular Imaging of Cardiovascular Diseases by Iron Oxide Nanoparticles. *Arterioscler. Thromb. Vasc. Biol.* **2021**, *41*, 601–613. [[CrossRef](#)] [[PubMed](#)]
24. Dikpati, A.; Madgulkar, A.R.; Kshirsagar, S.J.; Chahal, A.S. Journal of Advanced Pharmaceutical Sciences Targeted Drug Delivery to CNS Using Nanoparticles. *J. Adv. Pharm. Sci.* **2012**, *2*, 179–191.
25. Ngema, L.M.; Adeyemi, S.A.; Marimuthu, T.; Ubanako, P.; Wamwangi, D.; Choonara, Y.E. Synthesis of Novel Conjugated Linoleic Acid (CLA)-Coated Superparamagnetic Iron Oxide Nanoparticles (SPIONs) for the Delivery of Paclitaxel with Enhanced In Vitro Anti-Proliferative Activity on A549 Lung Cancer Cells. *Pharmaceutics* **2022**, *14*, 829. [[CrossRef](#)]
26. Frenkel, J.; Dorfman, J. Spontaneous and Induced Magnetisation in Ferromagnetic Bodies. *Nature* **1930**, *126*, 274–275. [[CrossRef](#)]
27. Enriquez-Navas, P.M.; Garcia-Martin, M.L. Application of Inorganic Nanoparticles for Diagnosis Based on MRI. *Front. Nanosci.* **2012**, *4*, 233–245. [[CrossRef](#)]
28. Wang, Y.X.J.; Hussain, S.M.; Krestin, G.P. Superparamagnetic Iron Oxide Contrast Agents: Physicochemical Characteristics and Applications in MR Imaging. *Eur. Radiol.* **2001**, *11*, 2319–2331. [[CrossRef](#)]
29. Sjøgren, C.E.; Briley-Sæbø, K.; Hanson, M.; Johansson, C. Magnetic characterization of iron oxides for magnetic resonance imaging. *Magn. Reson. Med.* **1994**, *31*, 268–272. [[CrossRef](#)]
30. Yilmaz, A.; Dengler, M.A.; Van Der Kuip, H.; Yildiz, H.; Rösch, S.; Klumpp, S.; Klingel, K.; Kandolf, R.; Helluy, X.; Hiller, K.H.; et al. Imaging of Myocardial Infarction Using Ultrasmall Superparamagnetic Iron Oxide Nanoparticles: A Human Study Using a Multi-Parametric Cardiovascular Magnetic Resonance Imaging Approach. *Eur. Heart J.* **2013**, *34*, 462–475. [[CrossRef](#)]
31. Stirrat, C.G.; Alam, S.R.; MacGillivray, T.J.; Gray, C.D.; Dweck, M.R.; Raftis, J.; Jenkins, W.S.A.; Wallace, W.A.; Pessotto, R.; Lim, K.H.H.; et al. Ferumoxytol-Enhanced Magnetic Resonance Imaging Assessing Inflammation after Myocardial Infarction. *Heart* **2017**, *103*, 1528–1535. [[CrossRef](#)] [[PubMed](#)]

32. Montet-Abou, K.; Daire, J.L.; Hyacinthe, J.N.; Jorge-Costa, M.; Grosdemange, K.; MacH, F.; Petri-Fink, A.; Hofmann, H.; Morel, D.R.; Vallée, J.P.; et al. In Vivo Labelling of Resting Monocytes in the Reticuloendothelial System with Fluorescent Iron Oxide Nanoparticles Prior to Injury Reveals That They Are Mobilised to Infarcted Myocardium. *Eur. Heart J.* **2010**, *31*, 1410–1420. [[CrossRef](#)] [[PubMed](#)]
33. Yang, Y.; Yang, Y.; Yanasak, N.; Schumacher, A.; Hu, T.C.C. Temporal and Noninvasive Monitoring of Inflammatory-Cell Infiltration to Myocardial Infarction Sites Using Micrometer-Sized Iron Oxide Particles. *Magn. Reson. Med.* **2010**, *63*, 33–40. [[CrossRef](#)] [[PubMed](#)]
34. Alam, S.R.; Shah, A.S.V.; Richards, J.; Lang, N.N.; Barnes, G.; Joshi, N.; MacGillivray, T.; McKillop, G.; Mirsadraee, S.; Payne, J.; et al. Ultrasmall Superparamagnetic Particles of Iron Oxide in Patients with Acute Myocardial Infarction Early Clinical Experience. *Circ. Cardiovasc. Imaging* **2012**, *5*, 559–565. [[CrossRef](#)]
35. Stirrat, C.G.; Alam, S.R.; MacGillivray, T.J.; Gray, C.D.; Forsythe, R.; Dweck, M.R.; Payne, J.R.; Prasad, S.K.; Petrie, M.C.; Gardner, R.S.; et al. Ferumoxytol-Enhanced Magnetic Resonance Imaging Methodology and Normal Values at 1.5 and 3T. *J. Cardiovasc. Magn. Reson.* **2016**, *18*, 46. [[CrossRef](#)]
36. Tanimoto, A.; Oshio, K.; Suematsu, M.; Pouliquen, D.; Stark, D.D. Relaxation Effects of Clustered Particles. *J. Magn. Reson. Imaging* **2001**, *14*, 72–77. [[CrossRef](#)]
37. Finn, J.P.; Nguyen, K.L.; Han, F.; Zhou, Z.; Salusky, I.; Ayad, I.; Hu, P. Cardiovascular MRI with Ferumoxytol. *Clin. Radiol.* **2016**, *71*, 796–806. [[CrossRef](#)]
38. Bao, Y.; Sherwood, J.A.; Sun, Z. Magnetic iron oxide nanoparticles as T1 contrast agents for magnetic resonance imaging. *J. Mater. Chem. C* **2018**, *6*, 1280–1290. [[CrossRef](#)]
39. Simon, G.H.; Bauer, J.; Saborovski, O.; Fu, Y.; Corot, C.; Wendland, M.F.; Daldrup-Link, H.E. T1 and T2 Relaxivity of Intracellular and Extracellular USPIO at 1.5T and 3T Clinical MR Scanning. *Eur. Radiol.* **2006**, *16*, 738–745. [[CrossRef](#)]
40. Taktak, S.; Sosnovik, D.; Cima, M.J.; Weissleder, R.; Josephson, L. Multiparameter Magnetic Relaxation Switch Assays. *Anal. Chem.* **2007**, *79*, 8863–8869. [[CrossRef](#)]
41. Yilmaz, A.; Rösch, S.; Klingel, K.; Kandolf, R.; Helluy, X.; Hiller, K.H.; Jakob, P.M.; Sechtem, U. Magnetic Resonance Imaging (MRI) of Inflamed Myocardium Using Iron Oxide Nanoparticles in Patients with Acute Myocardial Infarction—Preliminary Results. *Int. J. Cardiol.* **2013**, *163*, 175–182. [[CrossRef](#)]
42. Alam, S.R.; Stirrat, C.; Spath, N.; Zamvar, V.; Pessotto, R.; Dweck, M.R.; Moore, C.; Semple, S.; El-Medany, A.; Manoharan, D.; et al. Myocardial Inflammation, Injury and Infarction during on-Pump Coronary Artery Bypass Graft Surgery. *J. Cardiothorac. Surg.* **2017**, *12*, 115. [[CrossRef](#)]
43. Eitel, I.; Lücke, C.; Grothoff, M.; Sareban, M.; Schuler, G.; Thiele, H.; Gutberlet, M. Inflammation in Takotsubo Cardiomyopathy: Insights from Cardiovascular Magnetic Resonance Imaging. *Eur. Radiol.* **2010**, *20*, 422–431. [[CrossRef](#)]
44. Scally, C.; Abbas, H.; Ahearn, T.; Srinivasan, J.; Mezincescu, A.; Rudd, A.; Spath, N.; Yucel-Finn, A.; Yucel, R.; Oldroyd, K.; et al. Myocardial and Systemic Inflammation in Acute Stress-Induced (Takotsubo) Cardiomyopathy. *Circulation* **2019**, *139*, 1581–1592. [[CrossRef](#)]
45. Stirrat, C.G.; Alam, S.R.; MacGillivray, T.J.; Gray, C.D.; Dweck, M.R.; Dibb, K.; Spath, N.; Payne, J.R.; Prasad, S.K.; Gardner, R.S.; et al. Ferumoxytol-Enhanced Magnetic Resonance Imaging in Acute Myocarditis. *Heart* **2018**, *104*, 300–305. [[CrossRef](#)]
46. Vasanawala, S.S.; Nguyen, K.L.; Hope, M.D.; Bridges, M.D.; Hope, T.A.; Reeder, S.B.; Bashir, M.R. Safety and Technique of Ferumoxytol Administration for MRI. *Magn. Reson. Med.* **2016**, *75*, 2107–2111. [[CrossRef](#)]
47. Nguyen, K.L.; Yoshida, T.; Kathuria-Prakash, N.; Zaki, I.H.; Varallyay, C.G.; Semple, S.I.; Saouaf, R.; Rigsby, C.K.; Stoumpos, S.; Whitehead, K.K.; et al. Multicenter Safety and Practice for Off-Label Diagnostic Use of Ferumoxytol in MRI. *Radiology* **2019**, *293*, 554–564. [[CrossRef](#)]
48. FDA Drug Safety Communication: FDA Strengthens Warnings and Changes Prescribing Instructions to Decrease the Risk of Serious Allergic Reactions with Anemia Drug Feraheme (Ferumoxytol)|FDA. Available online: <https://www.fda.gov/drugs/drug-safety-and-availability/fda-drug-safety-communication-fda-strengthens-warnings-and-changes-prescribing-instructions-decrease> (accessed on 10 April 2022).